

## **Electronic Supporting information (ESI)**

### **Near-Infrared Upconversion Luminescence Total Internal Reflection Platform for Quantitative Image Analysis**

Wanying Xia, Bo Ling, Lun Wang, Feng Gao\* and Hongqi Chen\*

Anhui Key Laboratory of Chemo-Biosensing, Key Laboratory of Functional Molecular Solids, Ministry of Education, College of Chemistry and Materials Science, Anhui Normal University, Wuhu 241000, PR China

\*Corresponding author: Feng Gao; Hongqi Chen

Email: fgao@ahnu.edu.cn; hq80chen@mail.ahnu.edu.cn

## EXPERIMENTAL SECTIONS.

**Materials and reagents.** All the chemicals were used without next-step treatment. These were: IR-783, gadolinium(III) acetate ( $C_6H_9O_6Gd \cdot XH_2O$ ), ytterbium(III) acetate hydrate ( $C_6H_9O_6Yb \cdot XH_2O$ ), yttrium(III) acetate hydrate ( $C_6H_9O_6Y \cdot XH_2O$ ) and thulium(III) acetate hydrate ( $C_6H_9O_6Tm \cdot XH_2O$ ) from Sigma-Aldrich; formic acid ( $CH_2O_2$ ), oleic acid (OA), 4-hydroxyphenylboronic acid, sodium hypochlorite solution ( $NaClO$ ), 1-octadecene (ODE), sodium hydroxide ( $NaOH$ ) and nitrosyltetrafluoroborate ( $NOBF_4$ ) acquired from Aladdin Reagent (China); sodium hydride ( $NaH$ ) from Adamas-beta Reagent, Co., Ltd. (China); ammonium fluoride ( $NH_4F$ ), methanol ( $CH_3OH$ ), N,N-dimethylformamide (DMF), toluene, ethanol, ether absolute and cyclohexane from Sinopharm (China); ultra-pure water (18.25 M $\Omega$ cm) was used throughout experiments.

**Instruments.** The size and morphology of materials were characterized by a Hitachi HT-7700 transmission electron microscope (TEM). The elementary compositions of the materials were measured by a scanning electron microscope (SEM, Hitachi S-8100) combined with an energy-dispersive X-ray (EDX) spectrometer. Absorption spectra data were measured with a U-3900 spectrophotometer (Hitachi). The phases of upconversion nanocrystals were characterized using a Bruker D<sub>8</sub> Discover X-ray diffractometer (XRD) with Cu tube for producing Cu-K $\alpha$  radiation ( $\lambda = 0.1458$  nm). The upconversion luminescence spectra were recorded on a Hitachi F-4600 fluorescence spectrophotometer equipped with a 1.5 W 980 nm laser. The infrared spectra were recorded from a KBr window on an IRPrestige-21 spectrometer (SHIMADZU). The mass spectra (ESI-MS) data were acquired on an Agilent6220 mass spectrometer. Fluorescence decay curves were carried out on an Edinburgh Instruments FLS1000-stm luminescence spectrofluorimeter with the counting technique equipped under excitation at 980 nm.

**Preparation of the upconversion nanoparticles.** OA-capped  $NaGdF_4:Yb,Tm@NaYF_4$  core@shell nanoparticles were synthesized according to the reported method with slight modifications.<sup>1</sup>

**Synthesis of  $NaGdF_4:Yb,Tm$ .** First, 1 mL of 0.2 M  $C_6H_9O_6Gd \cdot XH_2O$ , 0.98 mL of 0.2 M  $C_6H_9O_6Yb \cdot XH_2O$  and 0.02 mL of 0.2 M  $C_6H_9O_6Tm \cdot XH_2O$  were placed in a 50 mL flask at room temperature. To the mixed solution was added 4 ml of oleic acid and 6 ml of 1-octadecene, which was then heated to 150 °C for 40 minutes, and then it was cooled down to room temperature with stirring. Next, 4.3 mL of methanol solution containing 1 mmol  $NaOH$  and 1.32 mmol  $NH_4F$  were fully mixed by using a vortex mixer, poured into the system immediately and stirred for 30 minutes at 50 °C. After that, the temperature was increased to 100 °C for degassing under an argon flow atmosphere to create an anhydrous and oxygen-free environment. Then the mixture was heated to 300 °C under argon atmosphere for 60 minutes and then cooled down. Finally, the core nanoparticles were rinsed with cyclohexane/ethanol (1:3, V/V) and collected by several cycles of centrifugation (8000 rpm, 3 minutes).

**Synthesis of  $NaGdF_4:Yb,Tm@NaYF_4$ .** First, a mixture of 2 mL of 0.2 M  $C_6H_9O_6Y \cdot XH_2O$ , 3 ml of oleic acid and 7 ml of 1-octadecene was heated to 150 °C for 40 minutes, and then cooled to room temperature with stirring. Next, 2 ml of cyclohexane solution containing  $NaGdF_4:Yb,Tm$  core nanoparticles was injected into the reaction solution. In addition, 4.3 mL of methanol solution containing 1 mmol  $NaOH$  and 1.32 mmol  $NH_4F$  were fully mixed by using a vortex mixer, immediately poured into the reaction system and stirred for

30 minutes at 50 °C. After that, the temperature was increased to 100 °C for degassing under an argon flow atmosphere to create an anhydrous and oxygen-free environment. Then the solution was heated to 300 °C under argon atmosphere for 60 minutes and then cooled down. Finally, the core-shell nanoparticles were rinsed with cyclohexane/ethanol (1:3, V/V) and collected by centrifugation (8000 rpm, 3 minutes) several times.

**Surface modification of UCNPs with NOBF<sub>4</sub>.** The NOBF<sub>4</sub> functionalized NaGdF<sub>4</sub>:Yb,Tm@NaYF<sub>4</sub>, named NOBF<sub>4</sub>-UCNPs, were prepared via a modified ligand exchange strategy as reported.<sup>2</sup> 5 mL of cyclohexane solution containing 40 mg of as-prepared core@shell UCNPs was added to a 5 mL N,N-dimethylformamide (DMF) solution of NOBF<sub>4</sub> (0.01 M). Then, the mixed solution was stirred for 15 minutes and the UCNPs were transferred from the upper cyclohexane layer to the bottom DMF layer. Afterwards, NOBF<sub>4</sub>-UCNPs were flocculated with cyclohexane/toluene (1:1, V/V), harvested by centrifugation (10000 rpm, 15 minutes), and rinsed two times with ultra-pure water. Finally, the NOBF<sub>4</sub>-UCNPs were redispersed in ultra-pure water.

**Synthesis of compound 1.** The synthesis of compound 1 is demonstrated in Scheme S1. The reaction was performed in a clean dry glass flask under N<sub>2</sub> atmosphere according to a modified previous method.<sup>3</sup> 4-Hydroxyphenylboronic acid (16.5516 mg, 0.12 mmol), IR-783 (37.0 mg, 0.05 mmol) and NaH (3.0 mg, 0.125 mmol) were mixed, and then 7 mL DMF solution was injected at room temperature. This reaction must be kept under N<sub>2</sub> atmosphere and away from light; it was stirred for 24 h. After drying under vacuum at 85 °C, DMF was evaporated thoroughly. In addition, the product was centrifuged and washed several times with ether absolute. Finally, it was vacuum-dried to yield compound 1.

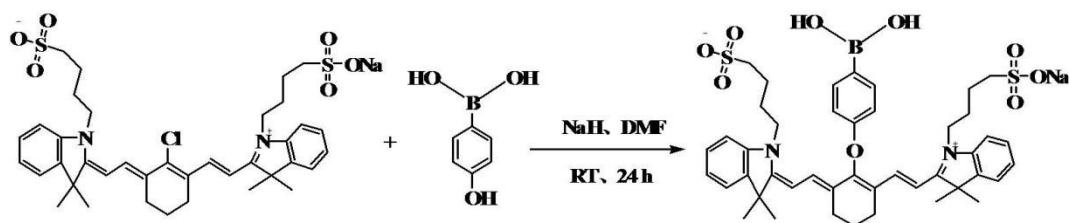
**Characterization.** To examine the phase and morphology of the as-synthesized NaGdF<sub>4</sub>:Yb,Tm@NaYF<sub>4</sub> UCNPs, X-ray diffraction and TEM techniques were utilized. In Fig. S2A and S2B, the TEM images show that the core and core@shell UCNPs are all well dispersed. The inset illustrated that the mean size of core@shell NaGdF<sub>4</sub>:Yb,Tm@NaYF<sub>4</sub> was ~31.57 nm, which was determined by the analysis of 100 randomly picked UCNPs. After modification, Fig. S2C reveals that the NOBF<sub>4</sub> functionalized nanoparticles are still very stable. Fig. S2D shows the XRD patterns, and all diffraction peaks of the UCNPs have a satisfactory match with the hexagonal phase structure NaGdF<sub>4</sub> (JCPDS 27-0699). Moreover, as Fig. S2E shows, the EDX spectrum displays the characteristic intensity curves of gadolinium, ytterbium, yttrium and thulium elements, also confirming the successful preparation of NaGdF<sub>4</sub>:Yb,Tm@NaYF<sub>4</sub> UCNPs. In the FT-IR spectrum, Fig. S2F(a), absorption bands of OA-UCNPs at 2927 and 2854 cm<sup>-1</sup> are ascribable to asymmetric and symmetric stretching vibrations of methylene (-CH<sub>2</sub>).<sup>4</sup> Meanwhile, the peaks occurring at 1465 and 1567 cm<sup>-1</sup> can be attributed to the vibrations of the carboxylic groups (-COO-).<sup>5</sup> After a ligand-exchange process, the stretching vibrations of methylene in the OA molecule in Fig. S2F(b) obviously decrease at 2800-3000 cm<sup>-1</sup>,<sup>6</sup> and a new peak at 1112 cm<sup>-1</sup> becomes visible, which comes from BF<sub>4</sub><sup>-</sup> ions.<sup>7</sup> These observations all indicate the successful surface modification of UCNPs with NOBF<sub>4</sub>. Another primary goal is characterizing the new synthetic cyanine dye. Herein, a detailed investigation of compound 1 has been completed via mass spectrometry and UV-vis absorption spectroscopy. As Fig. S3 shows, the molecular weight was investigated by mass spectrometry. MS: calculated for C<sub>44</sub>H<sub>53</sub>BN<sub>2</sub>O<sub>9</sub>S<sub>2</sub>: 827.3316;

found: 827.3836. Moreover, in Fig. S4B, compared to IR-783, one obvious feature is that the maximum absorption wavelength of compound 1 showed a blueshift of 13 nm (a: 793 nm, b: 780 nm). All of these observations support the hypothesis that the new dye has been synthesized successfully. In addition, the absorption spectra of compound 1 displayed a stepwise decrease in the presence of an increasing amount of  $\text{ClO}^-$ . Meanwhile, the reaction also accompanied by significant solution color change from green to yellow (Fig. S4E). A linear relationship (Fig. S4F) between the content of  $\text{ClO}^-$  over the range of 0-10  $\mu\text{M}$  and the absorbance was obtained ( $R^2 = 0.99$ ). The calibration curve was as follows:  $Abs. = -0.01904C + 0.4833$ , where  $Abs.$  was the absorbance of compound 1 in the presence of  $\text{ClO}^-$ . Hence, the absorbance of compound 1 was directly proportional to the concentration of  $\text{ClO}^-$ .

**Optimization of the assay.** To improve the detection efficiency of this method, it is necessary to optimize the corresponding experimental conditions with fluorescence spectrophotometer. A detailed analysis and discussion of three parameters that need to be considered in this work are presented, including compound 1 concentration, pH and time. These are elaborated below. Consider 80  $\mu\text{L}$  of  $\text{NOBF}_4$ -UCNPs in  $\text{H}_2\text{O}$  (2 mg/mL) in the system as an example. First, as mentioned earlier, the concentration of compound 1 is optimized to obtain a maximum quenching efficiency as in Fig. S5A. The results indicate that the optimum concentration of compound 1 for 0.16 mg/mL  $\text{NOBF}_4$ -UCNPs was 4.2  $\mu\text{g/mL}$ . The pH value of the system is of great significance in the application of fluorescent probes. So, the pH value is subsequently optimized. Fig. S5B reveals that the luminescence intensity of the nanoprobe UCNPs@DYE showed no significant differences in the pH range of 2.8 - 4.4, but as the amount of  $\text{ClO}^-$  was increased, there was a strong increase in upconversion luminescence under various pH values. Accordingly, pH = 3.8 was chosen as the optimal pH value. Furthermore, optimization of recovery time is not only essential to maximize recovery efficiency but can also validate the fact that this method has a quick response to  $\text{ClO}^-$ . Fig. S5C plots the time response curve. The luminescence intensity was enhanced immediately when  $\text{ClO}^-$  was added and reached a plateau at 6 minutes. Therefore, the optimal reaction time was 6 minutes.

**Procedures for detecting  $\text{ClO}^-$ .** First, the amount of compound 1 was optimized. Then, 80  $\mu\text{L}$  of  $\text{NOBF}_4$ -UCNPs in  $\text{H}_2\text{O}$  (2 mg/mL) was injected into a series of 2 mL centrifuge tubes. Then, various amounts of compound 1, which was redispersed in DMF, were added. After that, the volume was adjusted to 1 mL with  $\text{HCOOH-HCOONa}$  buffer solution (9 mM, pH 3.8) and mixed thoroughly with a shaker table. 15 minutes later, their luminescence spectra were recorded to get the optimum amount of compound 1. Next, 80  $\mu\text{L}$  of  $\text{NOBF}_4$ -UCNPs in  $\text{H}_2\text{O}$  (2 mg/mL) was injected in a series of 2 mL centrifuge tube. Then, the optimum amount of compound 1 was added and the mixture was incubated for 15 minutes at 25  $^\circ\text{C}$ . After that, various amounts of  $\text{ClO}^-$  were added and the volume was then adjusted to 1 mL with  $\text{HCOOH-HCOONa}$  buffer solution (9 mM, pH 3.8). After shaking for 6 minutes, their luminescence spectra were recorded.

**Quantitative detection of  $\text{ClO}^-$  based on imaging platform.** Glass coverslips with specifications of 24×50 mm were selected for treatment. They were ultrasonicated with household detergent for 10 minutes three times, after which they were dried in a drying oven. For each sample, only 10  $\mu\text{L}$  of that need to drip onto the coverslip.



Scheme S1. Synthesis of compound 1.

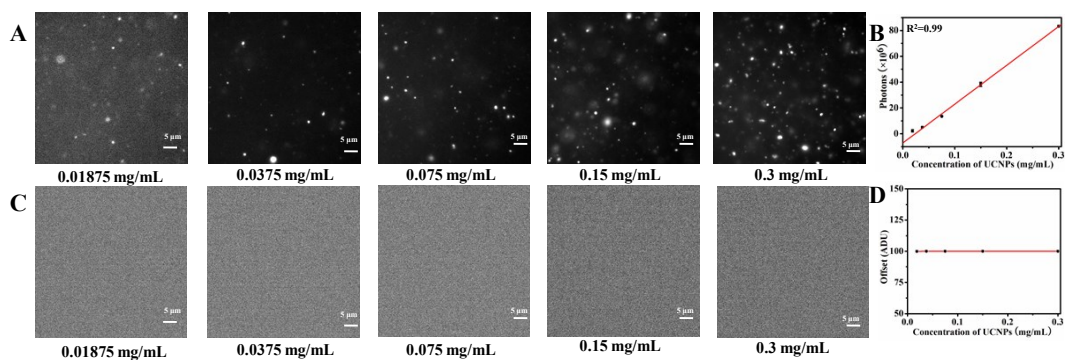


Fig. S1 (A) and (C) Luminescence images at various concentrations of UCNPs with and without 980 nm laser irradiation. (B) The relationship between the photons and the concentration of UCNPs with 980 nm laser irradiation. (D) The relationship between the offset and the concentration of UCNPs without 980 nm laser irradiation.

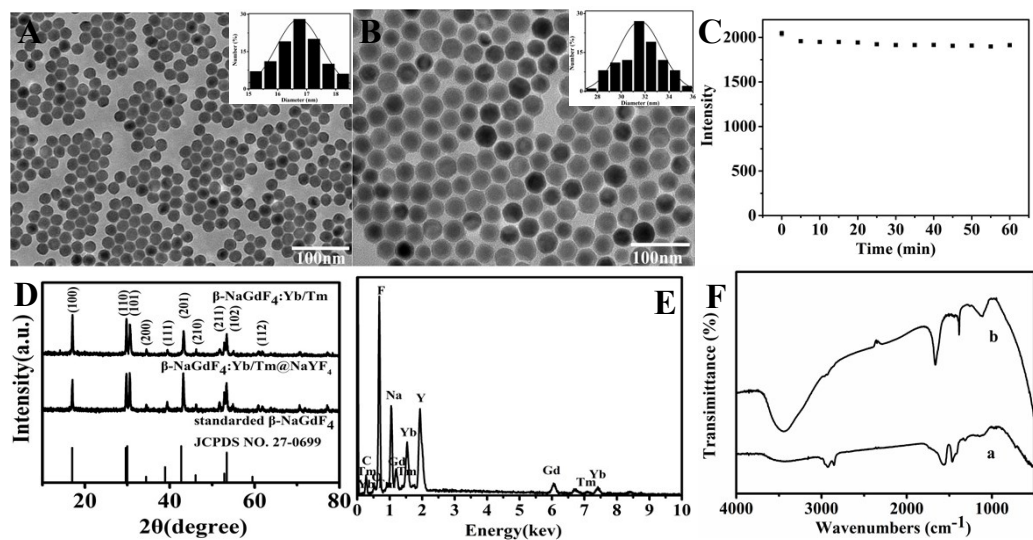
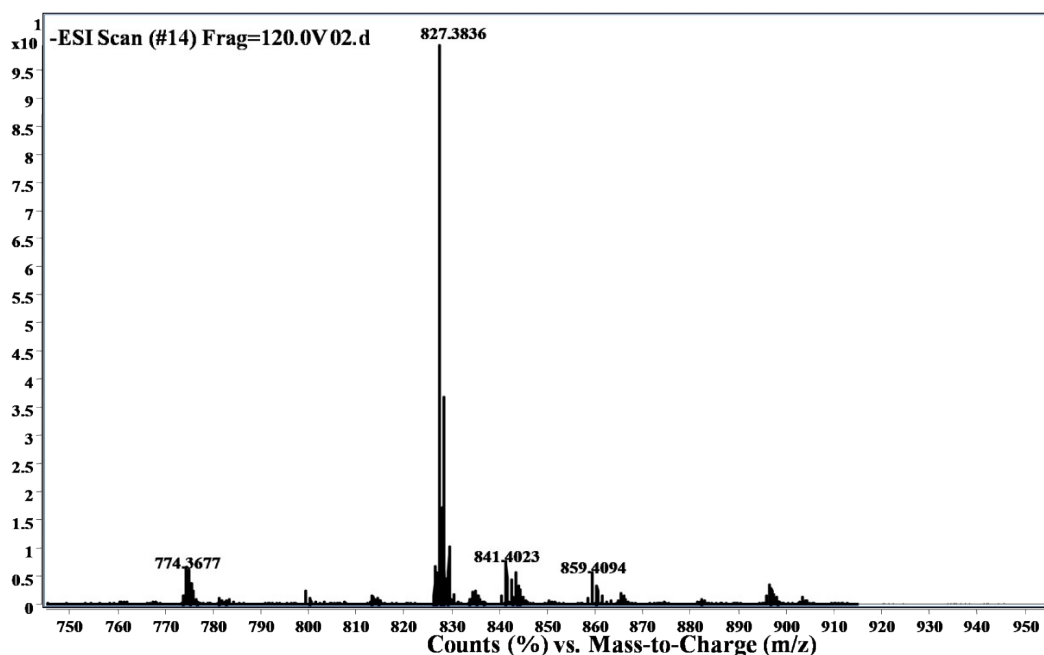
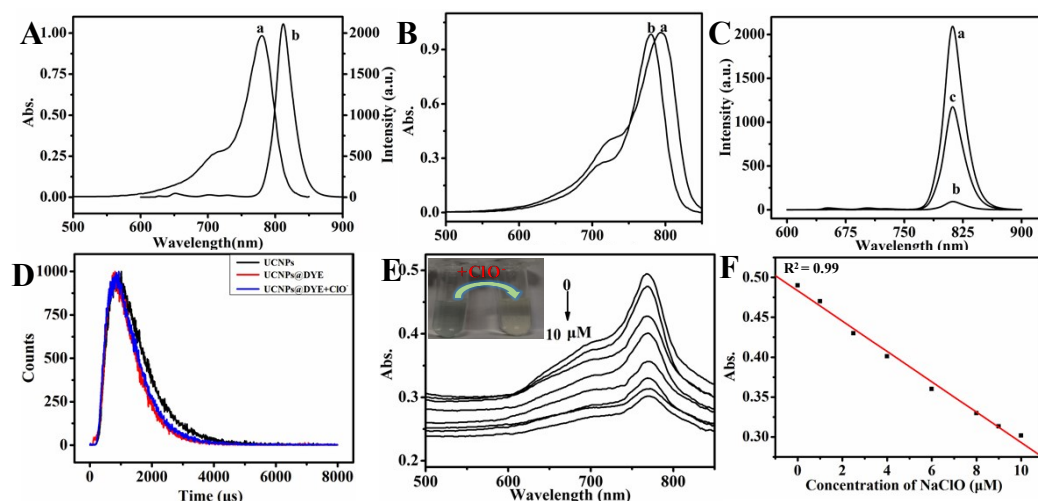


Fig. S2 (A and B) TEM micrographs of core UCNPs and core@shell UCNPs; the insets indicate size distributions; (C) The stability of the NOBF<sub>4</sub>-UCNPs; (D) Powder X-ray diffraction pattern of NaGdF<sub>4</sub>:Yb,Tm@NaYF<sub>4</sub> UCNPs (JCPDS 27-0699); (E) EDX spectrum of NaGdF<sub>4</sub>:Yb,Tm@NaYF<sub>4</sub> core@shell UCNPs; (F) FT-IR spectra of OA-capped UCNPs (a) and NOBF<sub>4</sub>-UCNPs (b).



**Fig. S3** HRMS spectrum of compound 1. MS: calculated for  $C_{44}H_{53}BN_2O_9S_2$ : 827.3316; found: 827.3836.



**Fig. S4** (A) Absorption spectrum of compound 1 (a) and the upconversion luminescence emission spectrum (b). (B) Absorption spectra of IR-783 (a) and compound 1 (b) in DMF, a blueshift of 13 nm (a: 793 nm, b: 780 nm). (C) Luminescence emission spectra of the UCNPs (a), UCNPs@DYE (b) and UCNPs@DYE+ClO<sup>-</sup> (c). (D) Luminescence decay curves of the emission at 812 nm of UCNPs (794  $\mu$ s), UCNPs@DYE (591  $\mu$ s) and UCNPs@DYE+ClO<sup>-</sup> (645  $\mu$ s) excited by a 980 nm laser. (E) Absorption spectra with the optimal amounts of compound 1 while adding different concentrations of ClO<sup>-</sup>. The inset shows the color change of compound 1 solution upon addition of ClO<sup>-</sup>. (F) The relationship between the ClO<sup>-</sup> concentrations and the absorbance of compound 1.

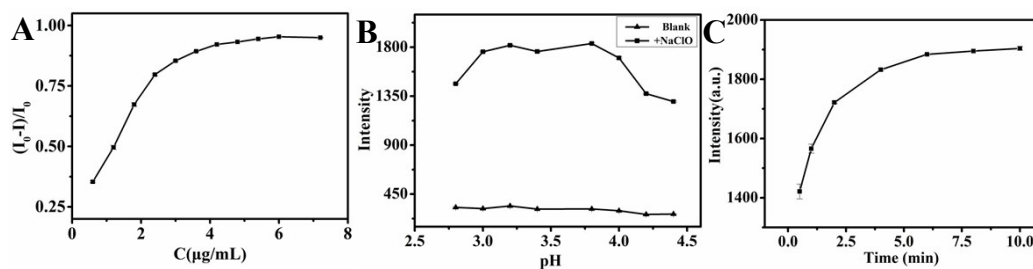


**Fig. S5** (A) 0.16 mg/mL NOBF<sub>4</sub>-UCNPs luminescence quenching efficiency with different concentrations of compound 1 ( $I$  was the intensity in the presence of compound 1 while  $I_0$  was with no compound 1); (B) The upconversion luminescence intensity changes in the presence and absence of ClO<sup>-</sup> at 10  $\mu\text{M}$  in HCOOH-HCOONa buffer solution (9 mM) at various pH values with 4.2  $\mu\text{g/mL}$  compound 1 present; (C) The upconversion luminescence intensity changes in the presence of 4.2  $\mu\text{g/mL}$  compound 1 after adding 10  $\mu\text{M}$  ClO<sup>-</sup> in HCOOH-HCOONa buffer solution (9 mM, pH 3.8) at different times.

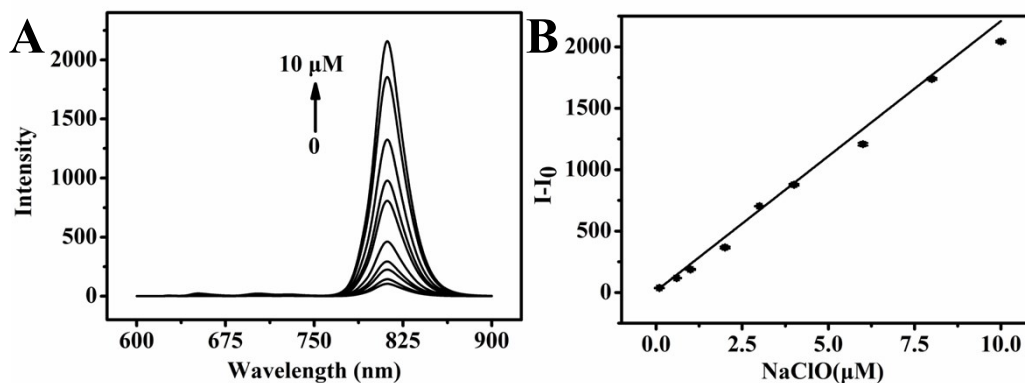


**Fig. S6** (A) The upconversion luminescence spectra with the optimal amounts of compound 1 while adding different concentrations of ClO<sup>-</sup>. (B) The fitted calibration curve for luminescence intensity at 812 nm with ClO<sup>-</sup> concentration.

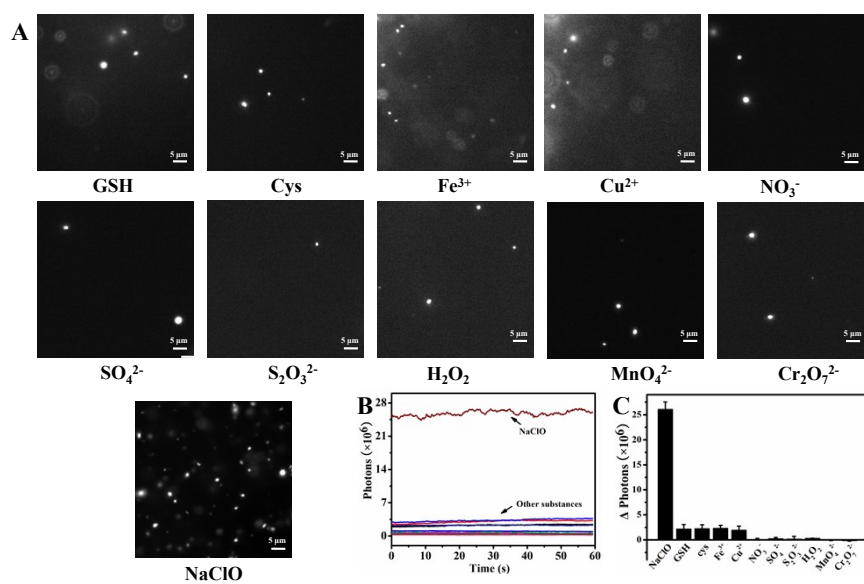


**Fig. S7** Luminescence images of selectivity of UCNPs@DYE toward ClO<sup>-</sup>. The interfering coexisting substances were all at a concentration of 5 μM.

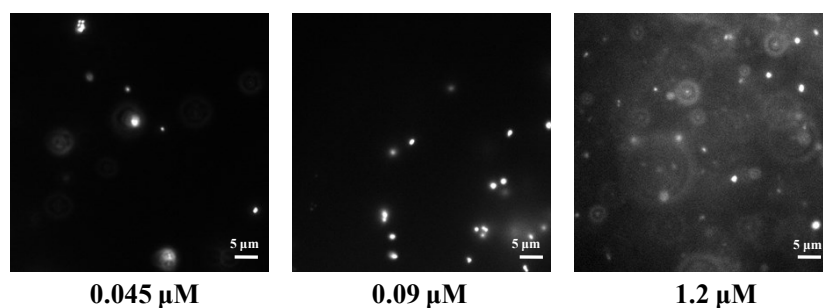


**Fig. S8** Luminescence images of the detection of ClO<sup>-</sup> in serum samples.

**Table S1.** Comparison of the different probes for determination of ClO<sup>-</sup>.

Probes	Linear range (μM)	LOD (nM)	References
Gal-NPA	0-1	460	8
Cy-FPA	0-9	700	9
mCDs@[Ru(bpy) <sub>3</sub> ] <sup>+</sup>	0.05-7	12	10
UCNPs@DYE	0.02-10	2.3	This work

**Table S2. Detection of ClO<sup>-</sup> in serum samples.**

Samples	Added ( $\mu\text{M}$ )	Detected ( $\mu\text{M}$ )	Recovery (%)
1	0.045	0.044	97.92
2	0.09	0.089	98.85
3	1.2	1.197	99.78

### Reference

1. F. Wang, R. Deng and X. Liu, *Nature Protocols*, 2014, **9**, 1634-1644.
2. A. Dong, X. Ye, J. Chen, Y. Kang, T. Gordon, J. M. Kikkawa and C. B. Murray, *Journal of the American Chemical Society*, 2011, **133**, 998-1006.
3. G. Chen, J. Damasco, H. Qiu, W. Shao, T. Y. Ohulchanskyy, R. R. Valiev, X. Wu, G. Han, Y. Wang, C. Yang, H. Agren and P. N. Prasad, *Nano Letters*, 2015, **15**, 7400-7407.
4. A. Xia, Y. Deng, H. Shi, J. Hu, J. Zhang, S. Wu, Q. Chen, X. Huang and J. Shen, *Acs Applied Materials & Interfaces*, 2014, **6**, 18329-18336.
5. Y. Shi, B. Shi, A. V. E. Dass, Y. Lu, N. Sayyadi, L. Kautto, R. D. Willows, R. Chung, J. Piper, H. Nevalainen, B. Walsh, D. Jin and N. H. Packer, *Scientific Reports*, 2016, **6**, 37533.
6. R. Liu, D. Tu, Y. Liu, H. Zhu, R. Li, W. Zheng, E. Ma and X. Chen, *Nanoscale*, 2012, **4**, 4485-4491.
7. H.D.Lutz, J.Himmrich and M.Schmidt, *Journal of Alloys and Compounds*, 1996, **241**, 1-9.
8. Q. Duan, P. Jia, Z. Zhuang, C. Liu, X. Zhang, Z. Wang, W. Sheng, Z. Li, H. Zhu, B. Zhu and X. Zhang, *Analytical Chemistry*, 2019, **91**, 2163-2168.
9. M. Sun, H. Yu, H. Zhu, F. Ma, S. Zhang, D. Huang and S. Wang, *Analytical Chemistry*, 2014, **86**, 671-677.
10. Y. Zhan, F. Luo, L. Guo, B. Qiu, Y. Lin, J. Li, G. Chen and Z. Lin, *ACS Sensors*, 2017, **2**, 1684-1691.